

## Creation of Polar and Nonpolar Ultra-Long-Range Rydberg Molecules

Chris H. Greene

*Department of Physics and JILA, University of Colorado, Boulder, Colorado 80309-0440*

A. S. Dickinson\*

*JILA, University of Colorado, Boulder, Colorado 80309-0440*

H. R. Sadeghpour

*ITAMP, Harvard-Smithsonian Center for Astrophysics, 60 Garden Street, Cambridge, Massachusetts 02138*

(Received 19 May 2000)

We predict the existence of a ubiquitous class of long-range molecular Rydberg states, whose Born-Oppenheimer potential curves are oscillatory in nature. These oscillations reflect the nodal structure of the atomic Rydberg state wave functions. The temperature and density of atoms in a Bose-Einstein condensate are particularly favorable for the laser excitation of ultra-long-range vibrational bound states localized at internuclear distances in the range  $10^3$ – $10^5$  a.u. A surprising trilobitelike class of polar homonuclear diatomics should exhibit electric dipole moments in the kilodebye range.

PACS numbers: 31.50.+w, 03.75.Fi, 33.80.Rv

The creation of dilute collections of ultracold atoms in magneto-optical traps, Bose-Einstein condensates (BECs), and optical lattices has made detailed spectroscopic investigation of molecules in unusual long-range states attached to the lower-lying  $s + p$  dissociation thresholds possible [1]. Rydberg molecules whose vibrational wave functions are shelved in shallow long-range wells ( $R \sim 20$ – $30$  a.u.) and stem from the interaction of Rydberg molecular potentials and the ion-pair formation potential curve, have been identified in two-photon spectroscopy [2]. The spectroscopy of long-range  $\text{Na}_2$  molecules trapped in a Born-Oppenheimer potential curve whose minimum occurs around 70 a.u., for instance, spawned an accurate confluence of experiment and theory that confirmed the retardation modification of the long-range interaction [3]. Other novel regimes include the frozen atomic Rydberg gas discussed independently by two different experimental groups [4], and the ultracold neutral plasma that has received attention even more recently [5]. Rydberg states of molecules at more conventional temperatures have been studied extensively in contexts such as line broadening [6].

The purpose of the present Letter is to discuss how the ultracold environment characteristic of modern-day Bose-Einstein condensates (BECs) should permit the efficient production of molecular Rydberg states whose vibrational levels are localized at internuclear distances of order  $\frac{3}{2}n^2$  Bohr radii, with  $n$  the principal quantum number. The formation of these states does not hinge on any of the coherence properties of a BEC, but a condensate provides particularly favorable regimes of temperature and density for their observation. The vibrational binding energies of these levels from  $n \approx 20$ – $50$  fall in the GHz or MHz range, for molecules excited out of a typical  $^{87}\text{Rb}$  atomic BEC. To our knowledge, these molecules would be the largest and most polar ever observed.

Two qualitatively different classes of molecular Rydberg states should be observable in an ultracold atomic gas. They are nonpolar or polar, respectively, depending on whether the electronic orbital angular momentum is low ( $l \leq 2$  for Rb) or high.

Rydberg molecules of the first class (*low l*) are formed from the interaction between a  $\text{Rb}(nl_j)$  Rydberg atom with low orbital angular momentum ( $l \leq 2$ ) and a distant Rb ground state atom. These molecules possess shallow Born-Oppenheimer potential curves that oscillate as a function of internuclear distance  $R$ . The oscillations mimic the behavior of the Rydberg electron radial wave function, with successive potential curve minima associated with successive maxima of the Rydberg electron density. In regions where the relevant energy-dependent  $e^-$ -Rb( $5s$ ) triplet scattering length  $A_T$  is negative, wave function antinodes generate minima in the Born-Oppenheimer potential curve.

Rydberg molecules of the second class (*perturbed hydrogenic states* [7]), arise from the coupling of the many quasidegenerate high- $l$  states whose quantum defects are negligible [7–10]. The Rydberg electron interaction with the core electrons results in a shift of the Rydberg energies from their unperturbed hydrogenic levels. Electrons in levels with large angular momenta remain sufficiently away from the core and their energies nearly coincide with those of atomic hydrogen. The perturbed hydrogenic potentials are far deeper than those of the low- $l$  type for comparable  $n$  and consequently support many more bound vibrational states. Each perturbed hydrogenic state also possesses a permanent electric dipole moment of magnitude  $D \approx R - \frac{1}{2}n^2$  a.u. (Atomic units are used except where stated otherwise.) To our knowledge, this is the only known case in which a homonuclear diatomic molecule is predicted to exhibit a permanent electric dipole moment. Such a huge electric dipole moment in any

long-lived molecular state presents an intriguing opportunity for manipulation and control through the application of an electric field or field gradient.

Throughout the present Letter, we adopt  $\text{Rb}_2$  as our prototype Rydberg molecule and demonstrate potential curves for states like  $\text{Rb}(nd_j) + \text{Rb}(5s)$  that display multiple minima at very large internuclear separations. The existence of these oscillatory extrema in such potential curves can be understood most simply through the use of a Fermi-type pseudopotential [8,11] to characterize the interaction between the atomic Rydberg electron and a ground state  $\text{Rb}(5s)$  atom. If  $\vec{r}$  is the position of the Rydberg electron relative to a  $\text{Rb}^+$  ground state ion, and  $\vec{R}$  is the position of the  $\text{Rb}(5s)$  atom relative to the ion, then the interaction potential can be taken, in a first approximation, as

$$V(\vec{r}, \vec{R}) = 2\pi A_T[k(R)]\delta(\vec{r} - \vec{R}). \quad (1)$$

Here  $A_T[k] \equiv -\tan\delta_0^T(k)/k$  is the energy-dependent triplet  $s$ -wave scattering length for electron collisions with ground state  $\text{Rb}(5s)$  atoms, defined in terms of the triplet  $s$ -wave phase shift  $\delta_0^T(k)$ . The relevant electron wave number  $k(R)$  is defined by the kinetic energy of the Rydberg electron at energy  $\varepsilon = -1/2n^2$  when it collides with a perturbing atom at a distance  $R$  from the  $\text{Rb}^+$  ion, namely,  $\frac{1}{2}k^2(R) = \varepsilon + 1/R$ . The accuracy of diatomic potential curves obtained within the Fermi model is improved [7,9,10] if an energy-dependent (and hence  $R$ -dependent) scattering length is adopted. We use the zero-energy scattering length  $A_T[0] = -16.05$  calculated by Bahrim *et al.* [12].

The negative value of the triplet scattering length implies that states of predominantly triplet character might be sufficiently attractive to produce bound vibrational states relative to the atomic dissociation threshold. Accordingly, we consider in this Letter only states that are controlled by the triplet scattering length. (The singlet value of Ref. [12] is  $A_S = 0.627$ , but it will not play a role in the calculations discussed here.) The energy dependence of  $A_T[k]$  has been determined from  $A_T[0]$  and the  $\text{Rb}(5s)$  polarizability,  $\alpha_{5s} = 319.2$  [13], using a generalized quantum defect theory [14], which is applicable over the entire relevant energy range.

When spin-orbit interactions can be neglected, the interesting  $^3\Sigma_g$  and  $^3\Sigma_u$  Born-Oppenheimer potential curves for  $\text{Rb}(nd) + \text{Rb}(5s)$  are both given in the Fermi model [11] by  $U(R) = E_{nd} + 2\pi A_T[k(R)]|\psi_{nd0}(\vec{R})|^2$ . This expression in terms of the unperturbed atomic Rydberg state wave function  $\psi_{nd0}$  results in highly oscillatory Born-Oppenheimer potential curves. Previous studies [7,9,10] showed that the Fermi pseudopotential description can largely reproduce the results of extensive *ab initio* calculations of diatomic potential curves, which adds to our confidence in this approach. A recent accurate *ab initio*

calculation of  $\text{LiH}$ ,  $\text{LiHe}$ , and  $\text{LiNe}$  potential curves has confirmed the existence of similar oscillations associated with atomic orbital undulations [15]. These oscillations are also seen in recent  $\text{NaH}$  calculations [16].

Figure 1(a) shows typical adiabatic potential curves associated with the low- $l$  class for  $\text{Rb}_2$  states of  $\Omega = 1$  symmetry in the vicinity of the  $30d_j + 5s$  dissociation thresholds. Here  $\Omega$  denotes the projection of the total electronic orbital plus spin angular momentum onto the internuclear axis. These molecular Rydberg states are best characterized in Hund's case (c), because the atomic spin-orbit splitting is larger than the electron-perturber interaction. While the oscillatory potential curves do track the radial Rydberg wave function, a surprising feature is the vanishing of the perturbation shift near  $R = 450$  a.u. In fact, this vanishing corresponds to the Ramsauer-Townsend zero of the  $^3S e^- - \text{Rb}(5s)$  phase shift at 0.042 eV (see, e.g., Fig. 4 of Ref. [12]).

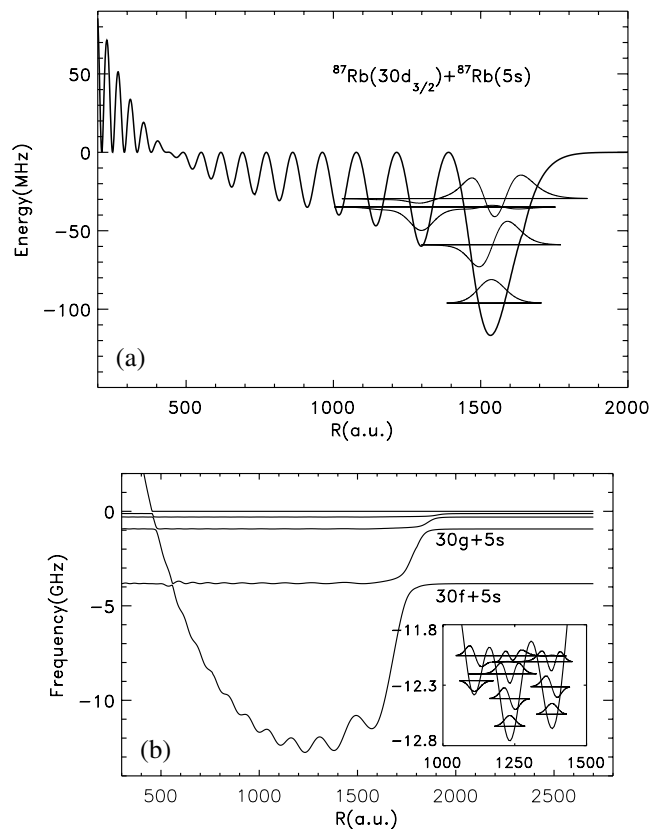


FIG. 1. (a) Typical Born-Oppenheimer potential curve for the low- $l$  class of molecular Rydberg states. The potential curve shown is predicted for the  $\text{Rb}_2$   $\Omega = 1$  molecular states formed from the  $30d_{j=3/2} + 5s$  states of the separated atoms and has predominantly triplet spin character. The lowest vibrational levels and their corresponding vibrational wave functions are also indicated. (b)  $^3\Sigma$   $\text{Rb}_2$  potential curves for the  $n = 30$  perturbed hydrogenic class of molecular Rydberg states. Several of the lowest vibrational levels are depicted in the inset. The zero of the energy scale in (b) is taken to be the energy of the degenerate hydrogenic manifold for  $n = 30$ .

Members of the low- $l$  class of molecular Rydberg states, such as the  $30d_j$  states in Fig. 1(a), exhibit shallow potential minima. The outermost potential well is approximately 120 MHz deep, and it supports approximately ten vibrational bound levels, three of which are indicated on the figure along with their radial wave functions. Attached to each  $nd$  dissociation threshold are additional potential curves that are not shown. Because these electronic states are dominated by  $\Pi$  or  $\Delta$  character and vanish on the internuclear axis, they remain unshifted from their atomic energies in this Fermi  $s$ -wave approximation.

While this molecular state has no net electric dipole moment, it has a huge polarizability of order  $n^7$  a.u. Modest laser power should produce these molecules in ample numbers. Also, in a typical condensate, the rate of inelastic transitions in the excited Rydberg level should be slow compared to the vibrational frequency.

The  $n = 30$  potential curve of the perturbed hydrogenic class is shown in Fig. 1(b), and its associated electronic wave function is presented in Fig. 2. Its striking nodal pattern is reminiscent of a trilobite. Interactions with the perturbing atom split away just one such state from the quasidegenerate manifold of high- $l$  states [7–10], which for Rb includes  $l \geq l_{\min} = 3$ . Neglecting the small quantum defects of all  $l \geq 3$  states, the lone perturbed adiabatic potential curve is given in terms of radial hydrogenic wave

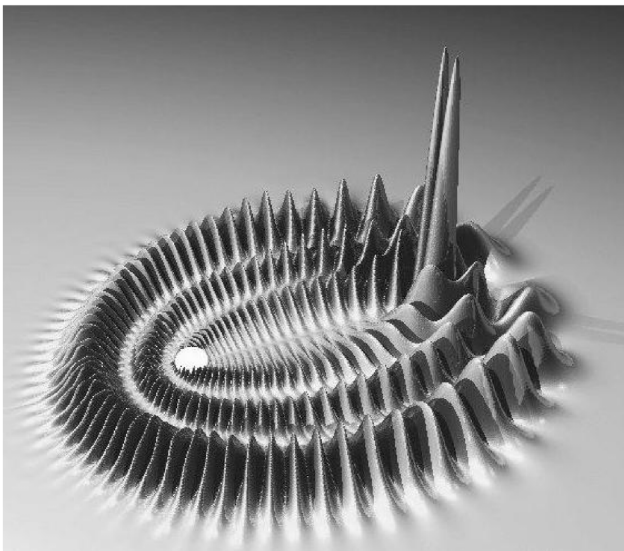


FIG. 2. A cylindrical coordinate surface plot of the electronic probability density,  $2\pi\rho|\psi(\rho, z, 0)|^2$  and  $2\pi\rho|\psi(\rho, z, \pi)|^2$ , is displayed for the lowest Born-Oppenheimer state shown in Fig. 1(b). This “trilobite-resembling” density corresponds to the equilibrium internuclear distance  $R = 1232$  a.u. for this  $n = 30$   $^3\Sigma$  perturbed hydrogenic state. The position of the Rb( $5s$ ) atom is directly underneath the “twin towers” centered at  $R = 1232$  toward the right side of the figure, while the Rb $^+$  ion is represented (with exaggerated size) as a small white sphere on the left. The region with appreciable density includes  $z \in [-700, 1700]$  and  $\rho \in [-1200, 1200]$ .

functions  $R_{nl}(R)$  evaluated at the location of the Rb( $5s$ ) perturber:

$$U_n(R) = -\frac{1}{2n^2} + 2\pi A_T[k(R)] \sum_{l=l_{\min}}^{n-1} \frac{2l+1}{4\pi} R_{nl}(R)^2. \quad (2)$$

This can be approximated [8] as  $U_n(R) \approx -1/(2n^2) + A_T[k(R)][2/R - 1/n^2 - (l_{\min} + \frac{1}{2})^2/R^2]^{1/2}/\pi n^3$ .

The perturbed hydrogenic potential curves are approximately 2 orders of magnitude deeper than their low- $l$  counterparts at  $n = 30$ . The low levels have roughly tenfold higher vibrational frequencies. The  $n = 30$  potential curve in Fig. 1(b) supports approximately 70 vibrational levels. The potential curve depths decrease with  $n$  as  $\approx -3.5 \times 10^5$  GHz/ $n^3$ . Moreover, in contrast to the low- $l$  class, the sum over degenerate states now includes functions with opposite electronic parities, which is why the electronic wave function now peaks close to the perturbing atom. This class of states has a large electric dipole moment,  $D \approx R - \frac{1}{2}n^2$  a.u. as mentioned earlier; the equilibrium value of  $R$  increases from 1232 a.u. at  $n = 30$  to about 3000 a.u. at  $n = 70$ , roughly linearly with  $n$ . This translates into  $D = 0.313$  kdebye (782 a.u.) for the states of Figs. 1(b) and 2.

Figure 3 proposes two different experiments to access these unusual molecular Rydberg states. One-photon excitation of an  $np_j$  level could also be replaced by a two-photon resonant or near-resonant process, to create a molecular Rb( $nd_j$ ) + Rb( $5s$ ) state of the type shown in Fig. 1(a). The electric dipole selection rule requires more photon steps to reach the degenerate hydrogenic (trilobite) states composed of high  $l \geq 3$ . Accordingly, the second experiment might use a microwave photon to induce a transition from a laser-excited  $nd$  state. Alternatively, application of a weak electric field might circumvent the dipole selection rule. Pulsed field ionization could be used to detect the excited Rydberg states.

One important question is whether the Fermi model can predict these Born-Oppenheimer potential curves to adequate accuracy. Previous calculations suggest that this is a reasonable assumption for the purposes of

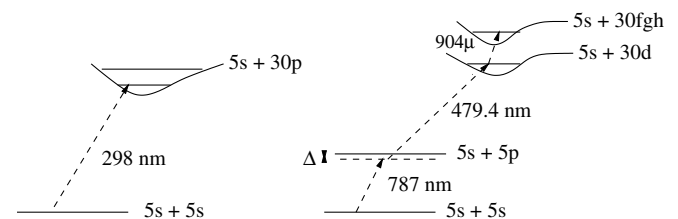


FIG. 3. Two experiments that could observe these different classes of molecular Rydberg states. The left one depicts a direct one-photon excitation of an  $np_j$  molecular state. The scheme on the right uses two photons to reach a high  $nd$  Rydberg state, followed by an additional microwave step to reach a perturbed hydrogenic state.

semiquantitative predictions, although it will be desirable to conduct more careful tests in the future. In fact, a shape resonance in the  $^3P^o$  symmetry for  $e^-$ -Rb( $5s$ ) scattering causes  $\tan\delta_{l=1}^T$  to diverge at a kinetic energy of 0.02 eV. Consequently, the relevant  $p$ -wave phase shift has already grown to equal that of the  $s$ -wave near the minimum of the lowest potential curve in Fig. 1(b), which corresponds to an electron kinetic energy of 0.007 eV. Consequently, the  $p$ -wave scattering is far more important than in previous applications of the Fermi pseudopotential. Omont's  $p$ -wave correction adds another term to the Fermi pseudopotential of Eq. (1) that has its general matrix elements given by  $\langle\psi_1|H^{p\text{-wave}}|\psi_2\rangle = -6\pi \tan\delta_{l=1}^T [k(R)] \nabla\psi_1(\vec{R}) \cdot \nabla\psi_2(\vec{R})/k(R)^3$ . The main effect is to cause a second attractive Born-Oppenheimer potential curve to split away from the degenerate hydrogenic manifold, but to lowest order it hardly affects the deepest potential of Fig. 1(b) because they cross diabatically. Eventually, at  $R \approx 700$ , where  $\tan\delta_{l=1}^T$  diverges to  $-\infty$ , this "correction" is unphysical and must be renormalized (see, e.g., Refs. [7,8]), but the decoupling suggests that our potential curves calculated within the  $s$ -wave Fermi approximation are substantially correct. Nevertheless, a desirable future goal will be to carry out more accurate model potential or pseudopotential calculations [17,18]. Out near the deepest  $R \approx 1520$  minimum of the  $30d_{3/2} + 5s(\Omega = 1)$  potential curve in Fig. 1(a), this state is little affected by the  $p$ -wave correction. It modifies them more substantially and qualitatively in the inner potential wells, however, notably at  $R < 1200$  a.u. where the  $^3P^o$   $e^-$ -Rb shape resonance plays a key role.

In virtually all homonuclear diatomic spectra studied to date, the charge clouds of the two atoms overlap appreciably, resulting in well-separated nonpolar gerade and ungerade states. For the unusual trilobitelike perturbed hydrogenic Rydberg states discussed here, however, the essentially exact degeneracy (splitting  $<10^{-100}$  a.u.) of gerade and ungerade states makes the  $g/u$  labels irrelevant. The resulting large permanent dipole moment is an unexpected property to find in a homonuclear molecule. For the  $n = 30$  example, even a stray field of order  $10 \mu\text{V}/\text{cm}$  can hybridize the  $J = 0$  and  $J = 1$  eigenstates of opposite total parity, owing to the combination of a large  $D = 782$  a.u., and a small rotational constant  $B \approx 10^{-11}$  a.u. [19]. The possibility of manipulating these fragile molecules is enhanced by their comparatively long radiative lifetimes, which we estimate to lie in the

0.1 msec range for the low- $l$  class and in the 10–100 msec range for the perturbed hydrogenic states around  $n = 30$ . Their existence in even higher  $n$ -manifolds opens the possibility of creating them at densities characteristic of a magneto-optical trap rather than in a BEC. In conclusion, we note that similar molecular states should exist in other alkali metal dimers and in general in atomic species for which the electron scattering length is negative. Such  $^3S$  scattering lengths are known to be negative for electron scattering from all ground state alkali metal atoms.

This work was supported in part by the National Science Foundation. We are indebted to C. Bahrim, U. Thumm, and I. I. Fabrikant for providing unpublished calculations of  $e^-$ -Rb scattering properties. We also thank J. Freeman and E. Snyder for technical assistance, and P. Gould and E. Eyler for stimulating discussions.

---

\*Permanent address: Physics Department, University of Newcastle, Newcastle upon Tyne, UK.

- [1] J. Weiner *et al.*, Rev. Mod. Phys. **71**, 1 (1999).
- [2] C.-C. Tsai, J. T. Bahns, and W. C. Stwalley, J. Chem. Phys. **100**, 768 (1994).
- [3] K. M. Jones *et al.*, Europhys. Lett. **35**, 85 (1996).
- [4] W. R. Anderson, J. R. Veale, and T. F. Gallagher, Phys. Rev. Lett. **80**, 249 (1998); I. Mourachko *et al.*, Phys. Rev. Lett. **80**, 253 (1998).
- [5] T. Killian *et al.*, Phys. Rev. Lett. **83**, 4776 (1999).
- [6] I. I. Fabrikant, J. Phys. B **19**, 1527 (1986); Comments At. Mol. Phys. **32**, 267 (1996).
- [7] Ning Yi Du and C. H. Greene, Phys. Rev. A **36**, 971 (1987); **36**, 5467(E) (1987); also J. Chem. Phys. **90**, 6347–6360 (1989).
- [8] A. Omont, J. Phys. (Paris) **38**, 1343 (1977).
- [9] E. de Prunelé, Phys. Rev. A **35**, 496 (1987).
- [10] F. Masnou-Seeuws and M. Dolan, J. Phys. B **17**, 2803 (1984); F. Masnou-Seeuws, J. Phys. B **15**, 883 (1982).
- [11] E. Fermi, Nuovo Cimento **11**, 157 (1934).
- [12] C. Bahrim and U. Thumm, Phys. Rev. A **61**, 022722 (2000); also C. Bahrim, U. Thumm, and I. I. Fabrikant (to be published).
- [13] R. W. Molof *et al.*, Phys. Rev. A **10**, 1131 (1974).
- [14] S. Watanabe and C. H. Greene, Phys. Rev. A **22**, 158 (1983).
- [15] A. Yiannopoulou *et al.*, Phys. Rev. A **59**, 1178 (1999).
- [16] T. Leininger *et al.*, J. Phys. B **33**, 1805 (2000).
- [17] J. Pascale, Phys. Rev. A **28**, 632 (1983).
- [18] J. Brust and C. H. Greene, Phys. Rev. A **56**, 2005 (1997).
- [19] J. M. Rost *et al.*, Phys. Rev. Lett. **68**, 1299 (1992).